Available online at www.sciencedirect.com
SCIENCE DIRECT®
Journal of Photochemistry and Photobiology A: Chemistry 163 (2004) 37–44
Journal of Photochemistry and Photobiology A:Chemistry
www.elsevier.com/locate/jphotochem

Comparison of Ag deposition effects on the photocatalytic activity of nanoparticulate TiO_2 under visible and UV light irradiation

Hyung Mi Sung-Suh, Jae Ran Choi, Hoe Jin Hah, Sang Man Koo*, Young Chan Bae*

Department of Chemical Engineering, College of Engineering, Hanyang University, Seoul 133-791, South Korea

Received 11 February 2003; received in revised form 21 May 2003; accepted 20 October 2003

Abstract

We investigated the photocatalytic degradation of rhodamine B (RB) dye in the aqueous suspensions of TiO_2 (~17 nm) and Ag-deposited TiO_2 nanoparticles under visible and UV light irradiation in order to evaluate and distinguish various effects of the Ag deposition on the TiO_2 photocatalytic activity. The TiO_2 and Ag–TiO_2 photocatalysts were characterized by XRD, TEM, XPS, UV-visible absorption and photon correlation spectroscopy. For comparison, the RB photodegradation was carried out in Degussa P25 TiO_2 and Ag-deposited P25 suspensions under the same condition. In the RB/Ag–TiO_2 system, Ag deposits significantly enhanced the RB photodegradation under visible light irradiation whereas the RB photodegradation under UV irradiation was slightly enhanced. The significant enhancement in the Ag–TiO_2 photoactivity under visible light irradiation can be ascribed to simultaneous effects of Ag deposits by both acting as electron traps and enhancing the RB adsorption on the Ag–TiO_2 surface.

Keywords: TiO_2; Ag deposition; Rhodamine B; Charge separation; Photodegradation; Visible light

1. Introduction

Photocatalytic degradation and mineralization of organic and inorganic pollutants on the semiconductor TiO_2 have been extensively studied in order to solve environmental problems relating to wastewaters and polluted air [1–8]. Among various metal oxide semiconductors, TiO_2 has been the focus of photocatalysts under UV irradiation because of its physical and chemical stability, low cost, ease of availability, non-toxicity, and electronic and optical properties. However, there are still basic problems to be solved for improving the photocatalytic activity of TiO_2. Because the semiconductor TiO_2 has a high band gap ($E_g > 3.2$ eV), it is excited only by UV light ($\lambda < 388$ nm) to inject electrons into the conduction band and to leave holes in the valence band [9]. Thus, this practically limits the use of sunlight or visible light as an irradiation source in photocatalytic reactions on TiO_2 [10]. In addition, the high rate of electron–hole recombination on TiO_2 particles results in a low efficiency of photocatalysis [11]. For the purpose of overcoming these limitations of TiO_2 as a photocatalyst, numerous studies have been recently performed to enhance electron–hole separation and to extend the absorption range of TiO_2 into the visible range. These studies include doping metal ions into the TiO_2 lattice [12,13], dye photosensitization on the TiO_2 surface [14–18], and deposition of noble metals [19–23].

In particular, noble metal-modified semiconductor nanoparticles become of current importance for maximizing the efficiency of photocatalytic reactions. The noble metals such as Pt [19,20] and Au [21,22] deposited or doped on TiO_2 have the high Schottky barriers among the metals and thus act as electron traps, facilitating electron–hole separation and promotes interfacial electron transfer process [24–27]. Most studies of noble metal-modified TiO_2 photocatalysts have focused on the details of the photoinduced electron transfer from the conduction band of UV-irradiated TiO_2 to noble metals for improving the photocatalytic activity of TiO_2 under UV irradiation. Only a few studies have been reported on visible light-induced photocatalytic reactions using noble metal-modified TiO_2 [28,29].

It is expected noble metals deposited on TiO_2 may show different effects on the photocatalytic activity depending on the wavelength of light illuminating photoreaction systems because the photocatalytic mechanism under UV irradiation

* Corresponding authors. Tel.: +82-2-2290-0527
(S.M. Koo)/+82-2-2290-0529 (Y.C. Bae); fax: +82-2-2281-4800
(S.M. Koo)/+82-2-2296-0568 (Y.C. Bae).
E-mail addresses: clarkhah@ihanyang.ac.kr, sangman@hanayng.ac.kr
(S.M. Koo), ycbae@hanayng.ac.kr (Y.C. Bae).

1010-6030/$ – see front matter © 2004 Elsevier B.V. All rights reserved.
doi:10.1016/S1010-6030(03)00428-3

is generally different from that under visible light irradiation. For example, in the photocatalytic degradation of dye on noble metal-deposited TiO_2 in the presence of O_2, TiO_2 acts as a photosensitizer as well as a photocatalyst under UV irradiation, but a dye acts as a photosensitizer as well as a degraded substrate under visible light irradiation. The charge separation within TiO_2 particles and subsequent electron transfer to O_2 for producing active oxygen radicals (e.g. $O_2^{\bullet -}$, $^{\bullet}OOH$, $^{\bullet}OH$) [15–17] are important to the efficiency of the dye photodegradation under both UV and visible light irradiation. The charge separation and subsequent electron transfer may be enhanced by noble metal deposition on TiO_2 particles, thereby improving the TiO_2 photocatalytic activity under both UV and visible light irradiation. Moreover, surface plasmon resonances of noble metal particles, which can be excited by visible light, increase the electric field around metal particles and thus enhance the surface electron excitation and electron–hole separation on noble metal-deposited TiO_2 particles [30–32].

Consequently, noble metals doped or deposited on TiO_2 are expected to show various effects on the photocatalytic activity of TiO_2 by the different mechanisms as follows that may act separately or simultaneously depending on the photoreaction conditions: noble metals (i) enhance the electron–hole separation by acting as electron traps, (ii) extend the light absorption into the visible range and enhance surface electron excitation by plasmon resonances excited by visible light, and (iii) modify the surface properties of photocatalyst.

Most studies of noble metal deposition on TiO_2 have been focused on group VIII metals using UV-irradiated photodegradation. Besides, some studies have reported contradictory results of the photodegradation of organic molecules on TiO_2 modified by Pt [19,20,33,34] or Ag [23,31] under UV irradiation. This is probably due to the type of TiO_2 used, photoreaction medium, the nature of organic molecules and their redox processes, and the metal content and dispersion [19]. Very few studies have concerned effects of the Ag deposition on the visible light-induced photocatalysis on TiO_2 [35]. Moreover, there has been no report to systematically investigate and distinguish the different roles of Ag deposits in the TiO_2 photocatalytic behavior under UV and visible light irradiation.

In this study, we examined the photocatalytic degradation of the rhodamine B (RB) dye in the aqueous suspensions of TiO_2 and Ag-deposited TiO_2 nanoparticles under visible and UV light irradiation in order to evaluate and distinguish the various effects of Ag deposits on the TiO_2 photocatalytic activity. The TiO_2 nanoparticles (~17 nm in size) was synthesized by the peptization method, and Ag metals were loaded on TiO_2 by photocatalytic deposition process. The activities of the synthesized TiO_2 and Ag-deposited TiO_2 were also compared to those of the commercial Degussa P25 TiO_2 and Ag-deposited P25 in the same photocatalytic condition. The experimental results are discussed by the different roles of Ag deposits in the RB photodegradation on TiO_2 photocatalyst through different mechanisms under visible and UV light irradiation.

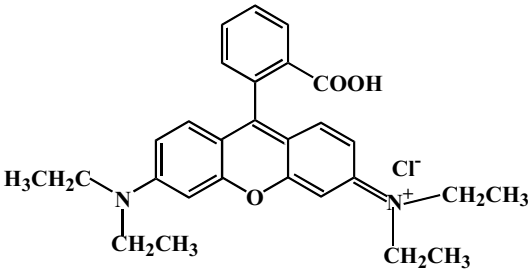

Fig. 1. The molecular structure of rhodamine B dye.

2. Experimental

2.1. Materials

Titanium isopropoxide (+97%) and silver nitrate ($AgNO_3$, analytical grade) were purchased from Aldrich and used as titanium and silver sources for the preparation of TiO_2 and Ag/TiO_2 photocatalysts. A commercial form of TiO_2 (P25, ca. 80% anatase, 20% rutile; BET area, ca. 50 m^2/g; primary size ~25–30 nm, agglomerate size ~100 nm) from Degussa was used for the comparison of the photocatalytic activity. Rhodamine B dye (*N*,*N*,*N*′,*N*′-tetraethylrhodamine, RB) obtained from Junsei was of analytical reagent grade and used without further purification. The structure of RB is shown in Fig. 1. Deionized and doubly distilled water was used for the preparation of all solutions.

2.2. Preparation of TiO_2 and Ag–TiO_2 photocatalysts

The nanoparticulate TiO_2 suspension (denoted as TiO_2 nanosol) was prepared by the peptization method. First, titanium isopropoxide (7.38 ml) was added dropwise to excess water with vigorous stirring at room temperature. The resulting gel was kept stirring for 1 h, and the solvent was then removed by filtration to leave a coagulated TiO_2 powder. In order to peptize the surface of the coagulated TiO_2 [36], the dry powder was added to water (40 ml) with vigorous stirring as adjusting pH to 3 by the addition of HNO_3. The mixture was then heated and aged at 60 °C for 6 h. The obtained TiO_2 nanosol (5 wt.% in TiO_2, pH 3) was transparent and stable for several months. The nanosol was further diluted with water to desired concentrations for the photocatalytic experiments. The TiO_2 concentration was 0.4 wt.% for the RB photodegradation under visible light irradiation and 0.04 wt.% under UV irradiation.

The suspension of metallic silver-deposited TiO_2 nanoparticles (Ag–TiO_2 nanosol) was prepared by a photocatalytic deposition process [37]. A desired volume of aqueous $AgNO_3$ solution (1.17×10^{-2} M) was added to the diluted

TiO_2 nanosol (50 ml). The mixture solution was then irradiated with UV light (100 W mercury lamp from Philips) for 30 min. The atomic ratio of Ag/Ti was calculated to be in a range of 1–10%.

2.3. Analytical methods

The crystalline phase of the synthesized TiO_2 nanoparticles was analyzed by X-ray powder diffraction (XRD) pattern using a Rigaku D/RAD-C diffractometer with Cu Kα radiation ($\lambda = 1.5418$ nm) at 40 kV and 100 mA. The average particle size of TiO_2 in the synthesized nanosol was measured by photon correlation spectroscopy (PCS) with an argon ion laser (Lexel Laser Inc. Model 95-2) operated at 514.4 nm and 200 mW. The TiO_2 nanosol was appropriately diluted with water for the light scattering experiment. The light scattered by particles was detected at 90° angle in respect to the incident beam. The optical property of the TiO_2 and Ag/TiO_2 nanoparticles was studied by UV-Vis absorption spectroscopy using a SCINCO S-2150 spectrophotometer. During the RB photodegradation, the RB concentration was also determined by the absorption spectroscopy. The Ag/TiO_2 particles were characterized by transmission electron microscopy (TEM) using a JEOL EM-2000EX II transmission electron microscope by applying a drop of the nanosol sample to the carbon-coated copper grid. To verify the presence of metallic silver deposited on TiO_2, a film made of the Ag–TiO_2 sample was examined by X-ray photoelectron spectroscopy (XPS) using a VG Scientific ESCALAB MKII spectrometer with Mg Kα line at 15 kV and 10 mA. The binding energy scale was calibrated to 284.6 eV for the main C 1s peak.

2.4. Measurements of photocatalytic activities

To investigate the effects of silver deposits on the photocatalytic activity of TiO_2, the oxidative photodegradation of RB was carried out in the aerated TiO_2 and Ag–TiO_2 nanosols under visible and UV light irradiation, respectively. A 100 ml pyrex beaker was used as a batch photoreactor. The TiO_2 or Ag/TiO_2 nanosol (50 ml) containing RB (10^{-5} M) was transferred into the photoreactor, and aerated with stirring for 30 min in the dark. The RB/nanosol was then irradiated with the lamp located above the reactor. The light sources purchased from Philips were a 200 W halogen lamp for visible light and a 100 W mercury lamp for UV. At given irradiation time intervals, a 1 ml-aliquot was taken from the RB/nanosol and analyzed by UV-visible absorption spectroscopy to monitor the degree of the RB photodegradation. The RB concentration was determined from the absorbance at a wavelength of 554 nm (λ_{max}). To compare the effects of silver deposits, the RB photodegradation was also performed in the commercial Degussa P25 TiO_2 and Ag-deposited P25 (Ag-P25) suspensions at the same experimental condition.

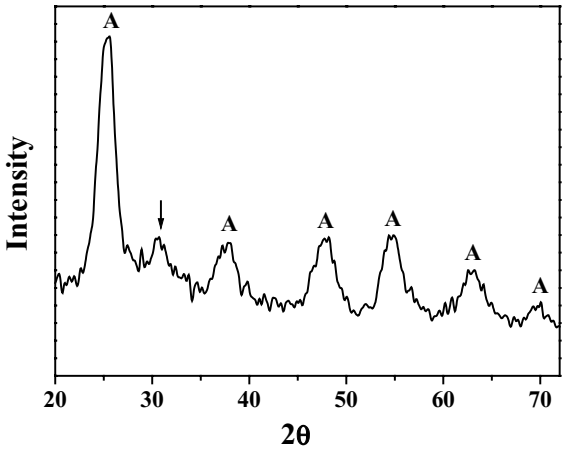

Fig. 2. XRD pattern of the synthesized TiO_2 sample. A: anatase phase. The peak marked with an arrow corresponds to the brookite phase.

3. Results and discussion

3.1. Characterization of TiO_2 and Ag–TiO_2 photocatalysts

The aqueous TiO_2 nanosol synthesized in this experiment was transparent and stable for several months. The crystalline phase of the TiO_2 sample was analyzed by XRD, and its XRD pattern is shown in Fig. 2. The TiO_2 sample consisted of mainly anatase with minor brookite phase [38] as indicated in the XRD pattern. The particle size of the TiO_2 sample was measured by PCS, and its particle size distribution is shown in Fig. 3. The TiO_2 sample had an average particle size of 17 nm with a narrow size distribution, indicating the TiO_2 nanoparticles were well dispersed in the synthesized nanosol although there were minor aggregates of ca. 50 nm, as can be seen in Fig. 3.

The valence state of silver in the Ag–TiO_2 sample was examined by XPS. The XP spectrum in Fig. 4 shows the characteristic Ag $3d_{5/2}$ peak that has a binding energy of 368 eV with a 6 eV splitting of the 3d doublet [39]. XPS peaks corresponding to Ag^+ ion were not found. This result confirms the presence of metallic silver deposits on the TiO_2

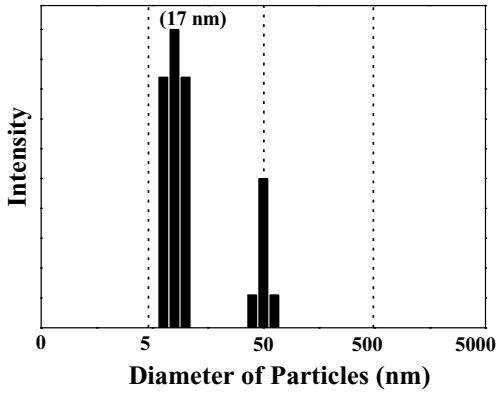

Fig. 3. The size distribution of the synthesized TiO_2 nanoparticles determined by photon correlation spectroscopy.

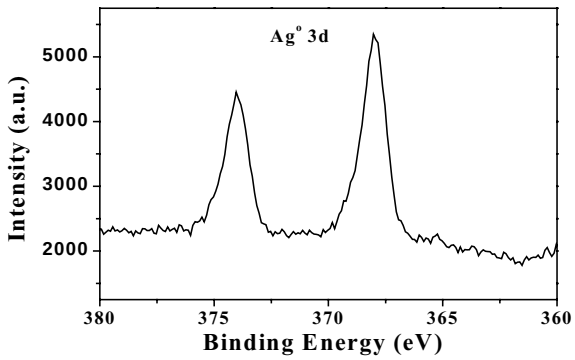

Fig. 4. XP spectrum for UV-irradiated Ag–TiO_2 sample.

surface of the Ag–TiO_2 sample irradiated with UV light. The size of Ag deposits on TiO_2 was determined from the TEM image shown in Fig. 5. The size varied with the Ag content in the TiO_2 nanosol. For the 2 at.% Ag–TiO_2 sample, Ag deposits were well dispersed on the TiO_2 particles with an average particle size of 2–4 nm as shown in Fig. 5. At higher silver content, formation of large Ag particles (>100 nm) was observed in the TEM image as similar to the previous report [23]. The Ag content and the particle size of Ag deposits may affect the photocatalytic activity of Ag–TiO_2 as discussed in the following section.

3.2. Comparison of photocatalytic activities of TiO_2 and Ag–TiO_2

3.2.1. RB photodegradation under visible light irradiation

Fig. 6 shows the spectral changes of RB in the TiO_2 nanosol under visible light irradiation. A decrease in the absorbance at 552 nm reflects the degradation of RB on the TiO_2 photocatalyst, thereby used as a measure of the photocatalytic activity. Compared to the pure TiO_2, the Ag–TiO_2 nanosol exhibited a significant increase in the RB photodegradation rate as shown in Figs. 7 and 8. It was found that the 2% Ag content was optimum to achieve the highest efficiency of the RB photodegradation for the TiO_2

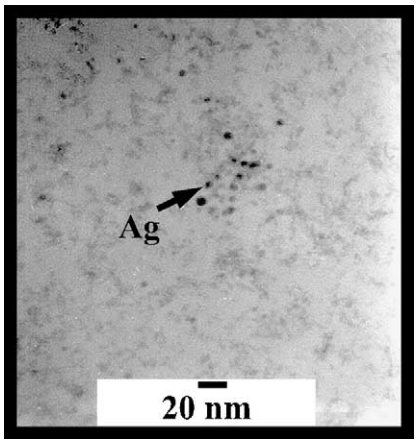

Fig. 5. TEM micrograph of 2 at.% Ag–TiO_2 sample.

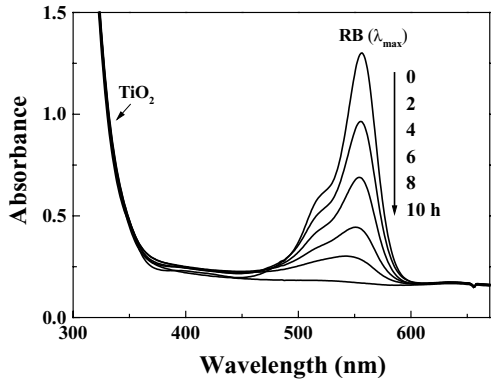

Fig. 6. Absorption spectral changes of RB in the TiO_2 nanosol as a function of irradiation time (visible light). The initial concentration (C_0) of RB was 1×10^{-5} M, and the TiO_2 content was 0.4 wt.%.

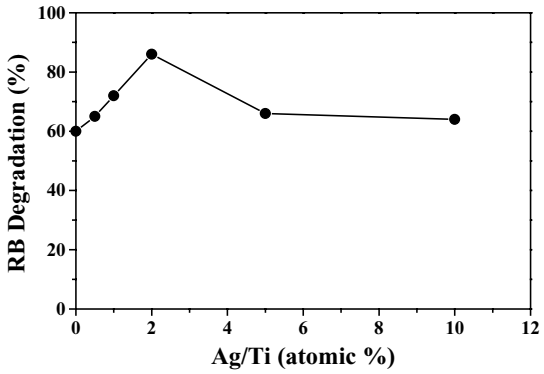

Fig. 7. Photocatalytic degradation of RB in Ag–TiO_2 nanosols as a function of the Ag content under visible light (4 h irradiation). The initial concentration (C_0) of RB was 1×10^{-5} M, and the TiO_2 content was 0.4 wt.%.

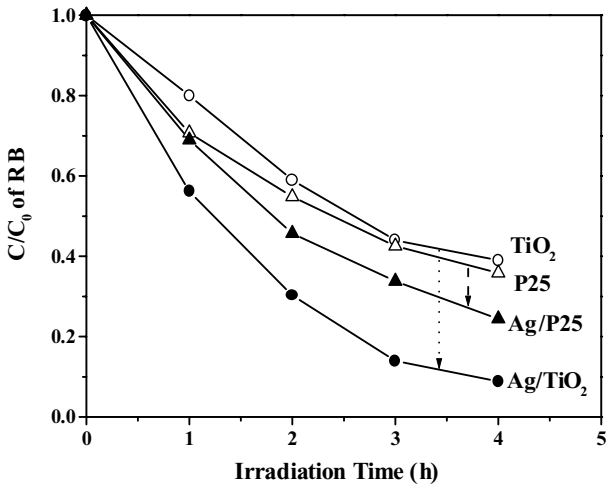

Fig. 8. Comparison of the RB photodegradation in TiO_2, Ag–TiO_2, P25, and Ag-P25 nanosols under visible light irradiation. The TiO_2 and Ag–TiO_2 nanosols were synthesized in this study. Ag-P25 was prepared from the commercial Degussa P25 titania. The initial concentration (C_0) of RB was 1×10^{-5} M. The TiO_2 content was 0.4 wt.%. The Ag contents was 2 at.%.

nanosols (Fig. 7). More Ag content could be detrimental to the photodegradation efficiency. It may be explained that at the Ag content below its optimum, the Ag particles deposited on the TiO_2 surface can act as electron–hole separation centers [25–27]. The electron transfer from the TiO_2 conduction band to metallic silver particles at the interface is thermodynamically possible because the Fermi level of TiO_2 is higher than that of silver metals [19]. This results in the formation of Schottky barrier at metal–semiconductor contact region, which improves the charge separation and thus enhances the photocatalytic activity of TiO_2. On the contrary, at the Ag content above its optimum, the Ag particles can also act as recombination centers, thereby decreasing the photocatalytic activity of TiO_2. It has been reported that the probability for the hole capture is increased by the large number of negatively charged Ag particles on TiO_2 at high Ag content, which reduces the efficiency of charge separation [19,23,29].

Under visible light irradiation, the Ag–TiO_2 sample showed a 30% increase in the RB photodegradation as compared to the pure TiO_2 (Fig. 8). In addition, the Ag–TiO_2 sample showed a higher photodegradation rate than both P25 and Ag-P25, although the pure TiO_2 sample had a slightly lower rate than P25 as shown in Fig. 8. By contrast, Ag-P25 exhibited only a 10% increase in the photodegradation as compared to P25. Accordingly, the Ag deposition was more beneficial to the photocatalytic activity of the synthesized TiO_2 than to P25 for the visible light-irradiated RB photodegradation. This probably results from a smaller particle size (∼17 nm) of the TiO_2 sample as compared the size (∼37 nm) of P25 analyzed by TEM and XRD [40]. The synthesized TiO_2 nanosol with smaller particles size and well dispersion is expected to provide a larger surface area for the RB adsorption and Ag dispersion on the TiO_2 surface, resulting in the higher photocatalytic activity of the Ag–TiO_2 sample as compared to that of Ag-P25.

The enhanced adsorption of RB on the Ag–TiO_2 surface can be inferred from a blue shift in λ_{max} of the RB absorption spectrum during its photodegradation as shown in Fig. 9. The Ag–TiO_2 sample showed a large decrease in the absorbance simultaneously with a large blue shift in λ_{max} during visible light irradiation. According to the previous results reported by Watanabe et al. [41] and Zhao and coworkers [15–17], the blue shift in λ_{max} of RB is caused by de-ethylation of RB occurring in competition with the degradation of the RB chromophore ring under visible light irradiation in CdS or TiO_2 suspensions. De-ethylation of RB is mainly a surface occurring reaction, whereas the RB degradation is predominantly a solution bulk process. RB is the *N*,*N*,*N*′,*N*′-tetraethylated rhodamine molecule showing λ_{max} at 552 nm. *N*,*N*,*N*′-Trietylated rhodamine has λ_{max} at 539 nm, *N*,*N*′-diethylated rhodamine at 522 nm, and *N*-ethylated rhodamine at 510 nm [41]. Accordingly, the large blue shift in λ_{max} of RB in the Ag–TiO_2 nanosol in Fig. 9(b) results from the significant de-ethylation of

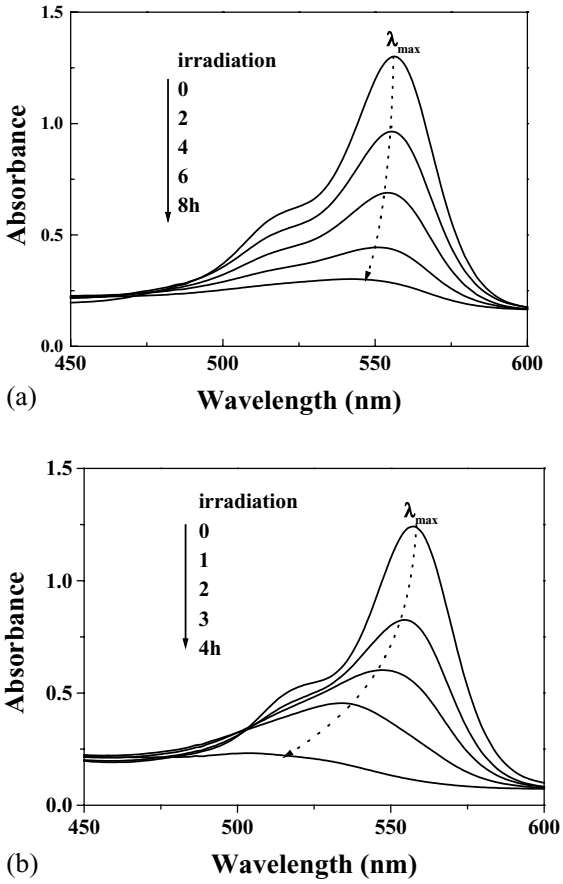

Fig. 9. Absorption spectral changes of RB in the (a) TiO_2 nanosol and (b) 2 at.% Ag–TiO_2 nanosol as a function of irradiation time (visible light). The dotted arrows indicate the blue shift in λ_{max} of RB during the photodegradation. The initial concentration (C_0) of RB was 1×10^{-5} M, and the TiO_2 content was 0.4 wt.%.

RB occurring on the surface of Ag–TiO_2 simultaneously with the degradation of the RB chromophore ring during visible light irradiation. This faster de-ethylation of RB on the Ag–TiO_2 surface may indicate that RB molecules can be more adsorbed on the Ag–TiO_2 surface than the TiO_2 surface, since de-ethylation of RB has been reported to be mainly a surface occurring reaction [16].

To compare the adsorption of RB molecules in TiO_2 and Ag–TiO_2 nanosols, the change in RB absorption spectra was monitored before and after adding the TiO_2 and Ag–TiO_2 samples in the dark as shown in Fig. 10. The decrease of the RB absorbance in Fig. 10 indicates that RB molecules acting as a photosensitizer under visible light irradiation are more pre-adsorbed on the Ag/TiO_2 surface than on the TiO_2 surface. About 5.4% of RB molecules were adsorbed on Ag/TiO_2 nanoparticles, whereas only 2.5% of RB molecules were adsorbed on TiO_2 nanoparticles. Therefore, under visible light irradiation, electron transfer from excited RB molecules to TiO_2 particles becomes more efficient in the Ag/TiO_2 nanosol, leading to the higher photocatalytic activity of Ag–TiO_2.

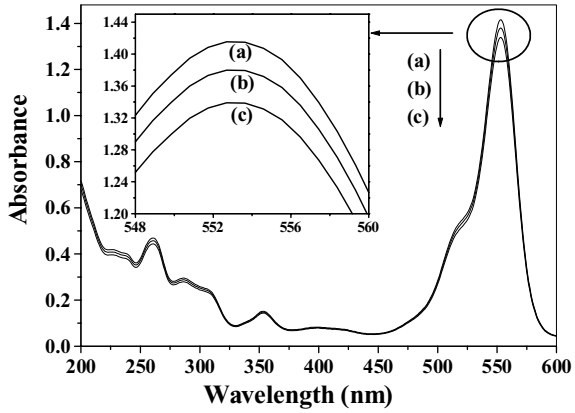

Fig. 10. Absorption spectra of RB before and after adsorption in TiO_2 and Ag–TiO_2 nanosol for 12 h in the dark: (a) initial RB solution (1×10^{-5} M), (b) after adsorption on TiO_2 and (c) after adsorption on Ag–TiO_2. The TiO_2 content was 0.4 wt.%. The Ag content was 2 at.%.

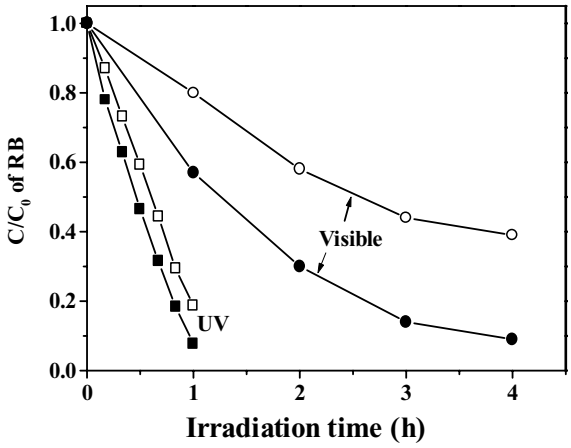

Fig. 12. Comparison of the RB photodegradation in the TiO_2 and 2 at.% Ag–TiO_2 nanosols under UV and visible light irradiation. The initial concentration (C_0) of RB was 1×10^{-5} M.

3.2.2. RB photodegradation under UV irradiation

Under UV irradiation, only 10% more RB photodegradation was achieved in the Ag–TiO_2 sample as compared to that in the TiO_2 sample (Fig. 11). Ag-P25 showed also 10% enhancement in the RB photodegradation than P25. The Ag–TiO_2 sample still showed a lower photodegradation rate than both P25 and Ag-P25, which is contrary to the result under visible light irradiation. The photocatalytic activities of both TiO_2 and Ag–TiO_2 were significantly lower than that of P25, probably resulting from the lower crystallinity of the TiO_2 sample that was not calcined in this experimental condition. This means that the Ag deposition on the TiO_2 sample does not overcome the lower crystallinity of the TiO_2 sample, thus slightly enhancing the RB photodegradation under UV irradiation.

Consequently, the beneficial effects of Ag deposition on the photocatalytic activity of the TiO_2 sample was more significant in the RB photodegradation under visible light irradiation than under UV irradiation, as can be seen in Fig. 12. Also, the Ag deposition was more beneficial to the synthesized TiO_2 sample than to P25 in the RB photodegradation under visible light irradiation (Fig. 9). These results may be ascribed to the different roles of Ag deposits in affecting the photocatalytic behaviors of TiO_2 under UV and visible light irradiation as discussed in the following.

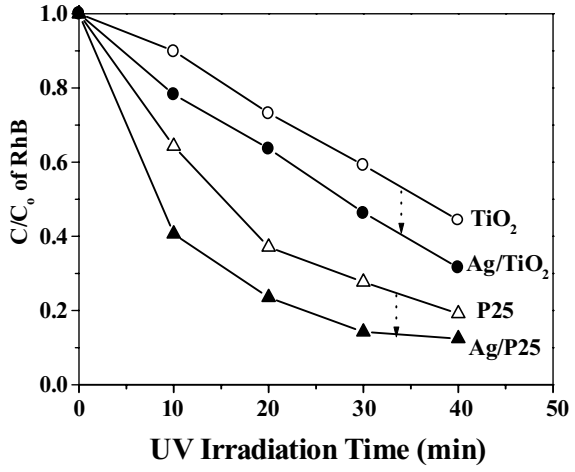

Fig. 11. Comparison of the RB photodegradation in TiO_2, Ag–TiO_2, P25, and Ag-P25 nanosols under UV irradiation. The initial concentration (C_0) of RB was 1×10^{-5} M. The TiO_2 content was 0.04 wt.%. The Ag content was 2 at.%.

3.3. Roles of Ag nanoparticles deposited on TiO_2

The photocatalytic activity of TiO_2 for the oxidative degradation of RB may be enhanced by the Ag deposition through the following mechanisms:

(1) Ag nanoparticles deposited on TiO_2 act as electron traps, enhancing the electron–hole separation and the subsequent transfer of the trapped electron to the adsorbed O_2 acting as an electron acceptor [24–27].
(2) More RB molecules are adsorbed on the surface of Ag–TiO_2 than on the TiO_2 surface, enhancing the photoexcited electron transfer from the visible-light sensitized RB to the conduction band of and subsequently increasing the electron transfer to the adsorbed O_2 (Figs. 9 and 10).
(3) The surface plasmon resonance of Ag particles is excited by visible light, facilitating the excitation of the surface electron and interfacial electron transfer [30–32].

In addition to these different roles of Ag deposits, the RB photodegradation in aqueous TiO_2 suspension has been shown to follow the different photocatalytic pathways under UV and visible light irradiation as shown in Fig. 13 [16,17,42]. Thus, we can estimate and distinguish various effects of Ag deposits on the TiO_2 photoactivity using the different mechanisms for the roles of Ag deposits and RB photocatalytic degradation.

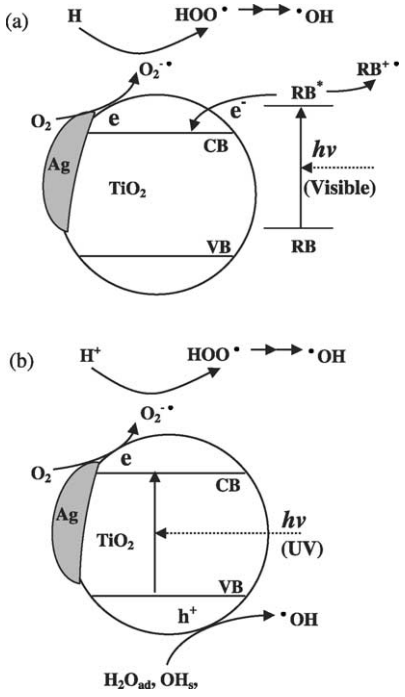

Fig. 13. Different photocatalytic pathways for the RB photodegradation on Ag–TiO_2 particles. (a) RB self-photosensitization pathway under visible light irradiation and (b) TiO_2-photosensitization pathway under UV irradiation.

3.3.1. Effects of Ag nanoparticles under visible light irradiation

The significantly enhanced photodegradation of RB in the Ag–TiO_2 nanosol under visible light irradiation (Fig. 12) may be ascribed to the cooperative roles of Ag deposits according to the three mechanisms mentioned above.

In the self-photosensitization pathway for the RB photodegradation on TiO_2 under visible light irradiation as shown in Fig. 13(a), RB, not TiO_2, is activated into its excited state at $\lambda > 470$ nm, injecting an electron into the conduction band (and/or surface states) of the TiO_2 semiconductor, whereas RB is converted to the cationic radical ($RB^{\bullet+}$). In turn, the injected electron on the TiO_2 particle reacts with adsorbed oxidants (usually O_2) to produce reactive oxygen radicals (e.g. $O_2^{\bullet-}$, $^{\bullet}OOH$, $^{\bullet}OH$). Subsequently, $RB^{\bullet+}$ is degraded or mineralized by these oxygen radicals. Under visible light irradiation, the semiconductor TiO_2 acts only as an electron-transfer mediator and the oxygen as an electron acceptor leading to an efficient separation of the injected electron and $RB^{\bullet+}$ (acting as a hole). Also, the rate-determining step in photocatalytic oxidations is believed to be the electron transfer from the TiO_2 surface to the adsorbed O_2 [23,43]. Consequently, the RB adsorption as well as charge separation is essential for the RB photodegradation on TiO_2 under visible light irradiation.

For the RB photodegradation on Ag–TiO_2 under visible light irradiation, the Ag particles on the TiO_2 surface can act as electron traps facilitating the electron–hole separation and subsequent electron transfer to the adsorbed O_2 according to the mechanism (1) [24–27].

For the mechanism (2), more RB molecules are adsorbed on the Ag–TiO_2 surface than on the TiO_2 surface, thus leading to more injection of the photoexcited electron from RB* to the conduction band of TiO_2 in self-photosensitization pathway under visible light irradiation as shown in Fig. 13(a). The enhanced RB adsorption on the Ag–TiO_2 surface can be supported by both the significant blue shift in λ_{max} of RB due to faster de-ethylation of RB on Ag–TiO_2 during the RB photodegradation (Fig. 9) and a decrease in the RB absorbance (λ_{max}) after contact with Ag–TiO_2 particles in the dark (Fig. 10).

For the mechanism (3), it has been reported that the surface plasmon resonance of Ag metals on TiO_2 is excited by visible light, enhancing the surface electron excitation and electron–hole separation [30–32]. Although we did not obtained the significant absorption band of the plasmon resonance in the Ag–TiO_2 sample due to the low Ag content and scattering of Ag–TiO_2 in this experimental condition, it is expected that the excitation of plasmon resonance may contribute to the enhancement in the photocatalytic activity under visible light irradiation, as reported for Au–TiO_2 [29] and Pt–TiO_2 [28].

In summary, we suggest that the cooperative effects of Ag deposits according to the three mechanisms lead to the significant enhancement in the TiO_2 photocatalytic activity under visible light irradiation as can be seen in Fig. 12.

3.3.2. Effects of Ag particles under UV irradiation

For the RB photodegradation on Ag–TiO_2 under UV irradiation, the Ag deposition slightly increases the TiO_2 photoactivity (Fig. 12). This may be ascribed to the effect of Ag deposits according to only the mechanism (1) under UV irradiation.

In a TiO_2-sensitization pathway for the RB photodegradation under UV irradiation as shown in Fig. 13(b), the valence electrons of TiO_2 particles are excited to the conduction band by UV light and after various other events, electrons on the TiO_2 particle surface are scavenged by the present molecular oxygen to produce reactive oxygen radicals, whereas the valence hole become trapped as the surface-bound $OH^{\bullet}$ radicals on oxidation of either the surface OH^- group and/or the surface H_2O molecules. Therefore, the charge separation on TiO_2 is a crucial factor to affect the efficiency of the RB photodegradation in TiO_2 under UV irradiation.

For the RB photodegradation on Ag–TiO_2 under UV irradiation, Ag metals act as electron traps according to the mechanism (1) thereby enhancing the charge separation. For the mechanism (2), however, it seems that the enhanced RB adsorption on the Ag/TiO_2 does not significantly contribute to enhancing the TiO_2 photoactivity under UV irradiation as much as under visible light irradiation, since RB molecules are not excited by UV light. Also, the effect of Ag deposits according to the mechanism (2) is not applicable under UV irradiation because the Ag surface plasmon resonance is not

excited by UV light. Consequently, only the mechanism (1) is applicable to the effect of Ag deposits thus leading to the slight increase in the Ag–TiO_2 photoactivity under UV irradiation (Fig. 12).

4. Conclusions

We have investigated the different roles of Ag deposits in enhancing the TiO_2 photocatalytic activity under UV and visible light irradiation. For comparison, the RB photodegradation was carried out in Degussa P25 titania and Ag-deposited P25 suspensions in the same photoreaction condition. The Ag–TiO_2 nanosol showed a 30% increase in the RB photodegradation under visible light irradiation, as compared to the pure TiO_2. The significant de-ethylation of RB occurs on the Ag–TiO_2 surface simultaneously with the degradation of its aromatic ring structure under visible light irradiation, indicating the enhanced RB adsorption on the Ag–TiO_2 surface. Under UV irradiation, however, the Ag/TiO_2 sample revealed only 10% more RB photodegradation as compared to the pure TiO_2. Under visible light irradiation, the significant enhancement in the Ag–TiO_2 photoactivity can be ascribed to simultaneous effects of Ag deposits by both acting as electron traps and enhancing the RB adsorption on the Ag–TiO_2 surface. Under UV irradiation, however, Ag deposits may exhibit the effect only as electron traps, thus leading to the slight enhancement in the Ag–TiO_2 photocatalytic activity.

Acknowledgements

This research was partially supported by the Brain Korea 21 Project in 2001. Authors also thank Korea Energy Management Corporation (KEMCO) for its financial support.

References

[1] M.R. Hoffmann, S.C. Martin, W. Choi, D.W. Bahnemann, Chem. Rev. 95 (1995) 69–96.
[2] A. Hogfelt, M. Gratzel, Chem. Rev. 95 (1995) 49–68.
[3] M.A. Fox, M.T. Dulay, Chem. Rev. 93 (1993) 341–357.
[4] E. Pelizzetti, N. Serpone, Photocatalysis–Fundamentals and Applications, Wiley, New York, 1989.
[5] A. Heller, Acc. Chem. Res. 28 (1995) 503–508.
[6] M. Anpo, H. Yamashita, in: M. Anpo (Ed.), Surface Photochemistry, Wiley, Chichester, 1996, pp. 117–164.
[7] P.V. Kamat, Chem. Rev. 93 (1993) 267–300.
[8] D.F. Ollis, H. Al-Ekabi, Photocatalytic Purification and Treatment of Water and Air, Elsevier, Amsterdam, 1993.
[9] C. Kormann, D.W. Bahnemann, M.R. Hoffmann, J. Phys. Chem. 92 (1988) 5196–5201.
[10] D.Y. Goswami, J. Sol. Energy 119 (1997) 101–107.
[11] A. Linsebigler, G. Lu, J.T. Yates, Chem. Rev. 95 (1995) 735–758.
[12] S.D. Mo, L.B. Lin, J. Phys. Chem. Solids 55 (1994) 1309–1313.
[13] W. Choi, A. Termin, M.R. Hoffmann, J. Phys. Chem. 98 (1994) 13669–13679.
[14] K. Vinodgopal, D.E. Wynkoop, P.V. Kamat, Environ. Sci. Technol. 30 (1996) 1660–1666.
[15] J. Zhao, T. Wu, K.Wu.K. Oikawa, H. Hidaka, N. Serpone, Environ. Sci. Technol. 32 (1998) 2394–2400.
[16] T. Wu, G. Liu, J. Zhao, H. Hidaka, N. Serpone, J. Phys. Chem. B 102 (1998) 5845–5851.
[17] G. Liu, T. Wu, T. Lin, J. Zhao, Environ. Sci. Technol. 33 (1999) 1379–1387.
[18] A. Fujishima, T.N. Rao, D.A. Tryk, J. Photochem. Photobiol. C: Photochem. Rev. 1 (2000) 1–21.
[19] A. Sclafani, J.-M. Herrmann, J. Photochem. Photobiol. A 113 (1998) 181–188.
[20] A. Wold, Chem. Mater. 5 (1993) 280–283.
[21] V. Subramanian, E. Wolf, P. Kamat, J. Phys. Chem. B 105 (2001) 11439–11446.
[22] C.Y. Wang, C.Y. Liu, X. Zheng, J. Chen, T. Shen, Colloid. Surf. A. 131 (1998) 271–280.
[23] V. Vamathevan, R. Amal, D. Beydoun, G. Low, S. McEvoy, J. Photochem. Photobiol. A 148 (2002) 233–245.
[24] J. Disdier, J.M. Herrmann, P. Pichat, J. Chem. Soc., Faraday Trans. I 77 (1981) 2815–2826.
[25] A. Henglein, J. Phys. Chem. 83 (1979) 2209–2216.
[26] J.-M. Herrmann, in: R.T.K. Baker, S.J. Tauster, J.A. Dumesic (Eds.), Strong Metal–Support Interactions, ACS Symposium. Series, vol. 298, 1986, pp. 200–211.
[27] J.-M. Herrmann, J. Disdier, P. Pichat, J. Phys. Chem. 90 (1986) 6028–6034.
[28] Y. Cho, W. Choi, J. Photochem. Photobiol. A 148 (2002) 129–135.
[29] X.Z. Li, F.B. Li, Environ. Sci. Technol. 35 (2001) 2381–2387.
[30] G. Zhao, H. Kozuka, T. Yoko, Thin Solid Films 277 (1996) 147–154.
[31] J.M. Herrmann, H. Tahiri, Y. Ait-Ichou, G. Lassaletta, A.R. Gonzales-Elipe, A. Fernandez, Appl. Catal. B 13 (1997) 219–228.
[32] G. Lassaletta, A.R. Gonzales-Elipe, A. Justo, A. Fernandez, F.J. Ager, M.A. Respaldiza, J.G. Soares, M.F. Da Silva, J. Mater. Sci. 31 (1996) 2325–2332.
[33] W. Mu, J.M. Herrmann, P. Pichat, Catal. Lett. 3 (1989) 73–84.
[34] G. Al-Sayyed, J.C. D'Oliveira, P. Pichat, J. Photochem. Photobiol. A 58 (1991) 99–114.
[35] E. Stathatos, T. Petrova, P. Lianos, Langmuir 17 (2001) 5025–5030.
[36] B.L. Bischoff, M.A. Anderson, Chem. Mater. 7 (1995) 1772–1778.
[37] J.-M. Herrmann, J. Disdier, P. Pichat, J. Catal. 113 (1988) 72–81.
[38] M. Loelsch, S. Cassaignon, J.F. Guillemoles, J.P. Jolivet, Thin Solid Films 403–404 (2002) 312–319.
[39] D. Briggs, M.P. Seah, Practical Surface Analysis, Wiley, New York, 1983.
[40] Z. Zhang, C.-C. Wang, R. Zakaria, J.Y. Ying, J. Phys. Chem. B 102 (1998) 10871–10878.
[41] T. Watanabe, T. Takizawa, K. Honda, J. Phys. Chem. 81 (1977) 1845–1851.
[42] P.V. Kamat, J. Phys. Chem. B 106 (2002) 7729–7744.
[43] Y. Li, G. Lu, S. Li, J. Photochem. Photobiol. A 152 (2002) 219–228.